

Article

Design and development of a two-color emissive FRET pair based on a photostable fluorescent deoxyuridine donor presenting a mega-Stokes shift

Nicolas P. F. Barthes, Krishna Gavvala, Dominique Bonhomme, Anne Sophie Dabert-Gay, Delphine Debayle, Yves Mély, Benoît Y. Michel, and Alain Burger

J. Org. Chem., **Just Accepted Manuscript** • DOI: 10.1021/acs.joc.6b01807 • Publication Date (Web): 10 Oct 2016

Downloaded from <http://pubs.acs.org> on October 10, 2016

Just Accepted

"Just Accepted" manuscripts have been peer-reviewed and accepted for publication. They are posted online prior to technical editing, formatting for publication and author proofing. The American Chemical Society provides "Just Accepted" as a free service to the research community to expedite the dissemination of scientific material as soon as possible after acceptance. "Just Accepted" manuscripts appear in full in PDF format accompanied by an HTML abstract. "Just Accepted" manuscripts have been fully peer reviewed, but should not be considered the official version of record. They are accessible to all readers and citable by the Digital Object Identifier (DOI®). "Just Accepted" is an optional service offered to authors. Therefore, the "Just Accepted" Web site may not include all articles that will be published in the journal. After a manuscript is technically edited and formatted, it will be removed from the "Just Accepted" Web site and published as an ASAP article. Note that technical editing may introduce minor changes to the manuscript text and/or graphics which could affect content, and all legal disclaimers and ethical guidelines that apply to the journal pertain. ACS cannot be held responsible for errors or consequences arising from the use of information contained in these "Just Accepted" manuscripts.



ACS Publications

Design and development of a two-color emissive FRET pair based on a photostable fluorescent deoxyuridine donor presenting a mega-Stokes shift

Nicolas P. F. Barthes,^a Krishna Gavvala,^b Dominique Bonhomme,^a Anne Sophie Dabert-Gay,^c Delphine Debayle,^c Yves Mély,^b Benoît Y. Michel,^{*a} Alain Burger^{*a}

a) Institut de Chimie de Nice, UMR 7272, Université de Nice Sophia Antipolis, CNRS, Parc Valrose, 06108 Nice Cedex 2, France

b) Laboratoire de Biophotonique et Pharmacologie, UMR 7213, Faculté de Pharmacie, Université de Strasbourg, CNRS, 74 Route du Rhin, 67401 Illkirch, France

c) Institut de Pharmacologie Moléculaire et Cellulaire, UMR 6097, Université de Nice Sophia Antipolis, CNRS, 660 Route des Lucioles, 06560 Valbonne, France

ABSTRACT: We report the synthesis and site-specific incorporation in oligodeoxynucleotides (ODNs) of an emissive deoxyuridine analog electronically conjugated on its C5-position with a 3-methoxychromone moiety acting as a fluorophore. When incorporated in ODNs, this fluorescent deoxyuridine analog exhibits remarkable photostability and good quantum yield. This deoxyuridine analog also displays a mega-Stokes shift, which allows its use as an efficient donor for FRET-based studies when paired with the yellow emissive indocarbocyanine Cy3 acceptor.

INTRODUCTION

Förster Resonance Energy Transfer (FRET) has become an inevitable technique in biology for determining structures, interactions and affinities between different partners from single molecules to cell imaging.¹ This process proved to be of particular interest in DNA research field due to its large domain of applications as for instance in hybridization technology and DNA-DNA/DNA-protein interaction studies.² On the other hand, DNA offers a unique platform for the design and construction of optimized emissive donor and acceptor dye pairs owing to its controllable structure and conformation.³

The emerging and most attractive way to develop FRET is to design donors exhibiting large Stokes shifts (i.e. >100 nm). Such fluorophores, named mega-Stokes shift dyes, turn out to be very appealing for FRET applications because they

prevent self-quenching and light scattering which reduce the signal background in imaging.⁴ The prototype of mega-Stokes shift dye is a push-pull fluorophore. It exhibits a larger dipole in the excited state due to intramolecular charge transfer (ICT) which results in a bathochromic shift of its emission band with increasing solvent polarity. But, for biological applications, such fluorophores should also have the following additional desired properties: absorption in the visible (>400 nm), high molar absorption coefficient (>30 000 M⁻¹.cm⁻¹), good fluorescence quantum yield (>40 %) and high photostability to avoid photobleaching. However, dyes that fulfill all these requirements are seldom encountered when incorporated in DNA.⁵ Indeed, incorporation of such fluorophores is inevitably accompanied by a significant quenching. In water, strong ICT dyes usually follow that trend: the larger the Stokes shift, the lower the quantum yield (e.g. pyridiniums,⁵ 4-aminophthalimide,^{6a,b} biaryllic 5-aminobenzoxazole,^{6c} DAN family members: 6-(dimethylamino)-2-naphthalenecarboxamide,^{6d,e} 2-ethynyl-6-cyanonaphthalene,^{6f} 5-amidodansyl^{6g}).

Recently, we have reported that the conjugate **1**, compiling a 3-methoxychromone electronically coupled to a dimethyluracil scaffold through a rigid ethynyl linker, absorbs strongly in the violet (35.000 M⁻¹.cm⁻¹), emits green light with large Stokes-shift ($\Delta\lambda$ = 100-135 nm) and exhibits appreciable fluorescence quantum yields in the range of 34 to 53 % in a set of protic and aprotic solvents. In contrast, the quantum yield was only 10 % in water (Figure 1).⁷ Anchoring the donor to the nucleobase through a short and rigid linker has an advantage to control the orientation and position of the emissive dipole as well as the distance separating it from the acceptor.

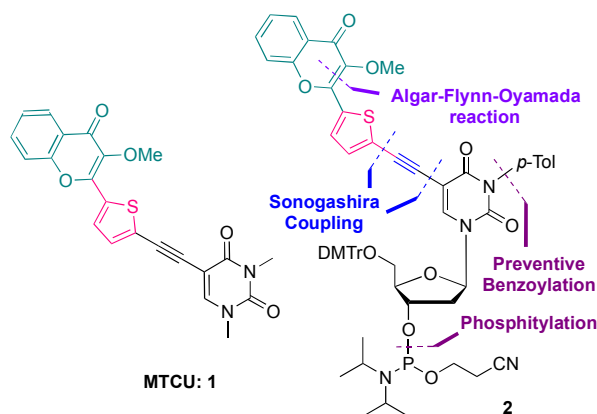


Figure 1. Fluorescent pyrimidine model **1** and retrosynthetic analysis of the targeted deoxyuridine amidite **2** incorporating methylated 3-hydroxychromone (3HC) fluorophore as a natural nucleobase modifier.

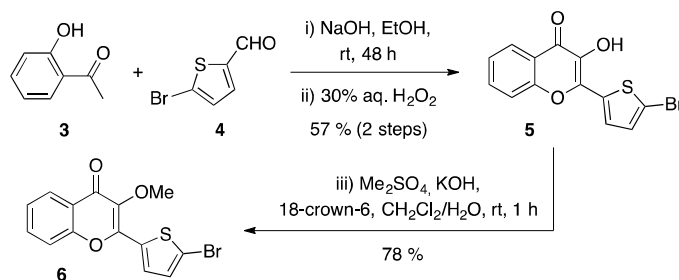
In this context, our research focused on the development of an efficient FRET pair as a ratiometric emitter for sensing interactions involving nucleic acids, by combining the fluorescent uracil derivative as a mega-Stokes shift donor with a 5'-terminal Cy3-acceptor.⁸ Herein, we report the synthesis of the corresponding fluorescent ethynyldeoxyuridine amidite **2** integrating the conjugated 3-methoxychromone fluorophore on its C5-position, its incorporation in DNA and the

characterization of the labeled sequences (Figure 1). We prove its site-specific labeling in ODNs and demonstrate that the properties of the mega-Stokes shift dye are highly appropriate for FRET applications.⁹

RESULTS AND DISCUSSION

Amidite retrosynthesis. The target fluorescent amidite **2** was obtained through a convergent strategy involving Sonogashira cross-couplings and Algar–Flynn–Oyamada reaction (Figure 1). As reported for the preparation of 3HC-conjugated deoxyuridine nucleosidic series,¹⁰ the synthetic approach is based on an unusual final assembly. Indeed, in spite of its competitive homo- and cross-couplings difficulties, it was favorable in terms of yield and purification to couple the electron-rich 5-ethynyldeoxyuridine with the electron-poor bromo-thienylchromones. By this strategy, it provided an access to **2** on a gram-scale via a 12-step pathway.

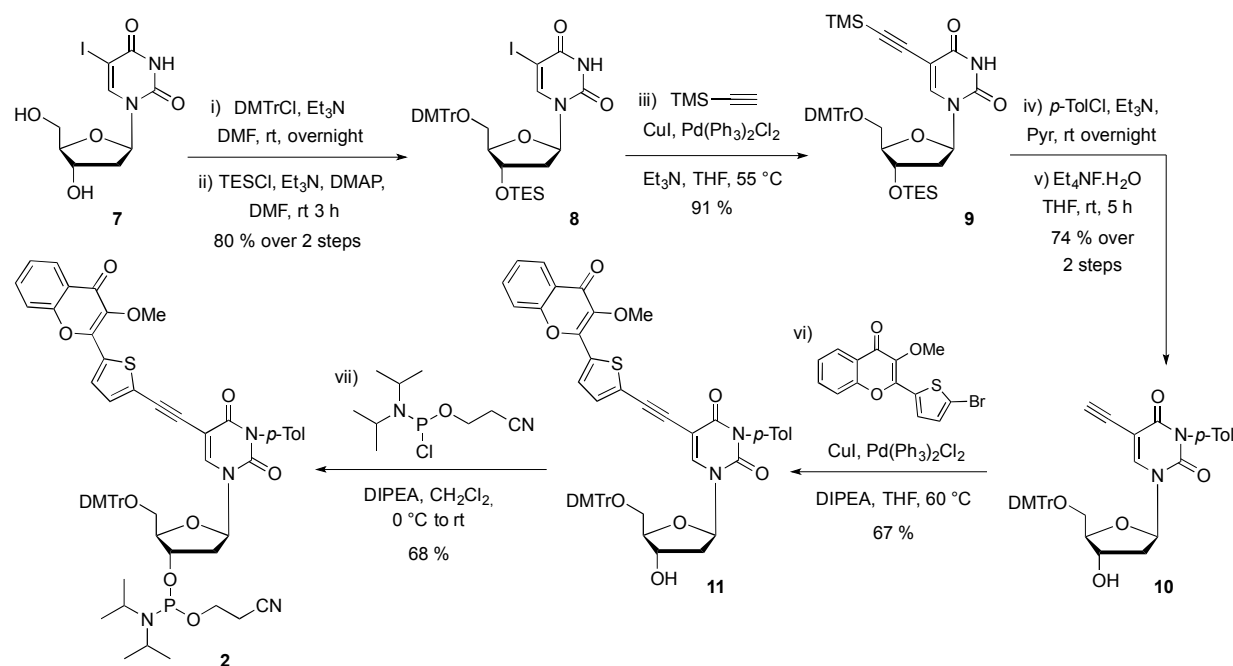
Amidite synthesis. The preparation of the 3HC fragment required for the final cross-coupling between the fluorophore and the nucleoside moieties, is depicted in Scheme 1. It involves a smooth and efficient Algar–Flynn–Oyamada process consisting of chalcone formation followed by oxidative cyclization. For that purpose, starting from 2-hydroxyacetophenone **3**, a Claisen–Schmidt condensation with carbaldehyde **4** in the presence of sodium hydroxide in ethanol followed by a treatment with aqueous hydrogen peroxide provided the 2-bromothieryl-3-hydroxychromone **5** in two-step yield (57%).¹¹ By using phase-transfer conditions (PTC), the reactive 3-hydroxyl group was then converted to a methyl ether **6**, facilitating the purification stages for all the downstream synthesis.¹²



Scheme 1. Synthetic preparation of the methylated 3HC fluorescent coupling partner **6**.

Concerning the preparation of the nucleosidic fragment required for the final assembly, we started from the readily available 5-iodo-deoxyuridine **7** (Scheme 2).¹³ Its 5'-hydroxyl group was first protected as an acid-labile trityl ether whereas the 3'-OH was consecutively masked by a triethylsilyl ether, using standard conditions for both reactions. Sonogashira coupling of the iodo intermediate **8** with TMS-acetylene supplied the protected ethynyl derivative **9** in high yields. We recently reported that a preventive toluoylation of the *N*3-imide of uracil moiety avoids competitive 5-*endo*-dig-cyclization during the further Pd-catalyzed coupling.^{10,14} To set up this base-labile imide protecting group, mild conditions (*p*-toluoyl chloride, Et₃N in pyridine) were employed.¹⁵ A subsequent treatment with the softly nucleophilic

tetraethylammonium fluoride monohydrate enabled to concomitantly cleave the TMS and TES silyl groups providing in satisfactory yields (71% over 2 steps) the terminal alkyne **10** as the building block for the ultimate assembly of the two fragments. A second Sonogashira reaction was then used for that purpose. Thus, when a standard catalytic system ($\text{PdCl}_2(\text{PPh}_3)_2$, CuI , Et_3N in THF) was employed, the reaction proceeded to give the coupled derivative **11** (67 % yield). Independently of the catalytic system being used, the sterically hindered Glaser coupling product was observed as a more polar spot by TLC (ca. 10-20 %). The desired fluorescent amidite **2** was then delivered pure in respectable yields under classical conditions.



Scheme 2. Synthesis of the modified deoxyuridine amidite **2** bearing a 3-methoxychromone scaffold as a fluorescent reporter.

ODN synthesis. Fluorescently-labeled 15-mer ODNs, incorporating site-selectively the amidite **2**, were efficiently obtained by solid-phase synthesis using standard procedures (SI). The sequences $d(\text{CGT TTT } \mathbf{XMX} \text{ TTT TGC})$, with $\mathbf{X} = \mathbf{T}, \mathbf{A}, \mathbf{C}$ or \mathbf{G} , were tagged with the conjugate **2** at the positions labeled **M**. The other ODNs required for the study were supplied from commercial sources. Complementary ODNs $d(\text{GCA AAA } \mathbf{YZY} \text{ AAA ACG})$, including \mathbf{Y} and $\mathbf{Z} = \mathbf{T}, \mathbf{A}, \mathbf{C}$ or \mathbf{G} , were annotated in italics. $d(\text{Cy3GCA AAA } \mathbf{YZY} \text{ AAA ACG})$ was labeled with Cy3 at the 5'-end (Figure S1).⁸ Control experiments were conducted with wild-type single strands $d(\text{CGT TTT } \mathbf{XTX} \text{ TTT TGC})$ where **T** replaces **M**. MS, HPLC & UV analysis confirmed the purity of the ODNs (Figures S2-S7; Table S1). For simplification, a 3-letter code corresponding to the 3 nucleotides marked in bold in the middle of the sequence was employed to specify the studied single strands (e.g. **AMA**) and double strands (e.g. **AMA-TTT**).

Photophysics. The labeled ODNs were chosen as model sequences to characterize the physical properties of the fluorophore **1** with respect to the nature of the flanking bases in single- (ss) and double-stranded (ds) DNAs (Table 1 & SI). The fluorescent emitter was located in the middle of the sequence rather than at the 5'-terminal positions of duplexes in order to avoid a sticky end association that could complicate the interpretation of the emission response.¹⁶ Melting temperature and CD experiments were first realized with the matched and mismatched labeled dsDNAs, and finally with the corresponding wild type sequences for comparison (Tables 1 and S2, Figures S8-S11). Thermal denaturation studies clearly demonstrated that the emissive T analog preferentially base-paired with A (Table S2, $\Delta T_m = +6.7$ to $+8.6^\circ\text{C}$ compared to mismatched pairs). Compared to the matched wild-type duplexes, the incorporation of **2** revealed to be slightly destabilizing ($\Delta T_m = -1.9$ to -6.8°C , Table S2, Figures S8-S9) but less than a mismatch ($\Delta T_m = -8.8$ to -11.3°C , Table S2). Comparable observations were commonly reported when a natural nucleoside was replaced with any nucleoside analogue bearing a hydrophobic fluorophore.²¹

Table 1. Spectroscopic data for labeled ODNs.^a

DNA	ss & ds samples	T_m ($^\circ\text{C}$) ^b	λ_{Abs} (nm) ^c	λ_{Em} (nm) ^d	Φ (%) ^e
1	TMT	-	399	500	30
2	TMT-AAA	45.2 (49.5)	392	490	50
3	AMA	-	399	498	21
4	AMA-TAT	43.1 (47.3)	392	491	47
5	CMC	-	398	500	24
6	CMC-GAG	46.5 (51.3)	392	491	6
7	GMG	-	400	498	2
8	GMG-CAC	51.4 (54.8)	392	491	1
9	AAA(Cy3)	-	548	565	18
10	TTT-AAA(Cy3)	51.9 (49.5)	548	564	20
11	TMT-AAA(Cy3)	47.5 (49.5)	396	564	-

a) Recorded at 20°C with $2\ \mu\text{M}$ of each ODN in buffer pH 7.0 (10 mM cacodylate buffer, 150 mM NaCl); b) Melting temperature (T_m) of the labeled matched duplex; T_m of the corresponding wild-type duplexes are listed in parentheses; $\pm 0.5^\circ\text{C}$; c) Position of the absorption maximum; $\pm 1\ \text{nm}$; d) Position of the emission maximum; $\pm 1\ \text{nm}$; e) Fluorescence quantum yields were determined by using the following standard references: quinine sulfate (QS) in $0.1\ \text{M}$ HCl solution ($\lambda_{\text{exc}} = 350\ \text{nm}$, $\Phi = 0.54$)¹⁷ and *p*-dimethylaminoflavone (dMAF) in EtOH ($\lambda_{\text{exc}} = 404\ \text{nm}$, $\Phi = 0.27$)¹⁸ for **M**; rhodamine 101 in EtOH ($\lambda_{\text{exc}} = 356\ \text{nm}$, $\Phi = 1.00$)¹⁹ for Cy3; $\pm 10\%$ mean standard deviation.

Furthermore, incorporation of the dye did not affect the secondary structure of the labeled DNA duplexes as evidenced by CD spectra, which confirmed a typical B-form signature (Figures S10-S11). The UV absorbance and fluorescence spectra of **1** in **DNA1-8** were recorded in phosphate buffer at pH 7.0 (Figures S12-S14). **DNA1-8** showed absorption maxima in the range of 392-400 nm (Table 1, Figure S12), indicating that the absorbance of the dye was marginally affected by the nature of the flanking bases in both ss and fully complementary dsDNAs. Compared to the free dye in solvents, the absorption of **M** was significantly red shifted ($\lambda_{\text{abs}} = 375$ nm in water),⁷ indicating that **M** may stack with the flanking bases in ODNs. The fluorescence emission maxima were located in the green region (ca. 500 nm), irrespective of the adjacent bases, conferring a mega-Stokes shift to the dye incorporated in DNA (98-103 nm, Table 1 and Figure S14). Remarkably, compared to the quantum yield reported for **1** in H₂O (10 %), the fluorophore displayed 2 to 5-fold enhanced quantum yields in **DNA1-5** (ca. 21-50 %). This increase in quantum yield might be due to the exposition of the fluorophore in a less hydrated environment.^{10,21} In contrast to **A**, **T** and **C** bases, the fluorophore is quenched by proximal **G** bases due to their well-known quenching behavior.²²

Photostability. Photostability of fluorescent dyes is a major concern in imaging applications and single molecule fluorescence spectroscopy. We therefore investigated the photodegradation of the free dye **1** and its incorporated form in ss and matched ds **DNA1-8** (Figures 2 and S15) under continuous illumination of the sample. For comparison, the *p*-dimethylamino-3-hydroxyflavone (dMAF), a known unstable push-pull fluorophore was also studied (Figure 2).²³ The curves were fitted with an exponential decay (Figure S16) to extract the time constants (τ_d) of photodegradation.

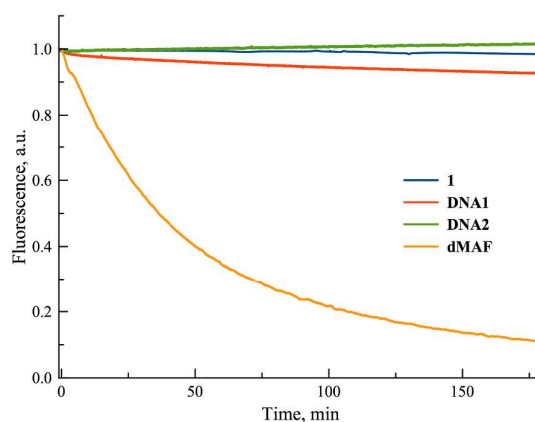


Figure 2. Photodegradation curves of fluorophore **1** in water (blue), ss **DNA1** (red) and ds **DNA2** (green) in buffer pH 7, and dMAF (yellow) in EtOH. Concentration of each sample was 2 μ M. Excitation was at 400 nm.

Dye **1** exhibits high photostability in its free form and when it is incorporated in DNA compared to its known analogue, dMAF (Figure 2 and S15). The photobleaching curve of dMAF exhibits a mono-exponential decay with τ_d of 47 min whereas **1** reveals to be photostable even after 180 min of illumination. This indicates that the methoxy group at position

3 of the chromone in **1** prevents photodegradation as it was observed for the methoxy derivative of dMAF.²⁴ ss **DNA1** shows a bi-exponential curve with τ_d values of 5 min and 3 h, whereas no degradation was noticed over a period of 3 h in ds **DNA2**. The bi-exponential nature in ss **DNA1** may be attributed to the existence of two populations with one exposed to water and the other being inside DNA. This heterogeneity was absent for ds **DNA2**, suggesting that the controlled exposition of the dye to the major groove in the duplex leads to enhanced photostability. To sum up, our data demonstrate that the dye fulfills the desired requirements to be a prospective candidate as a mega-Stokes shift FRET donor²² ($\lambda_{\text{Abs}} = 390\text{-}400\text{ nm}$, $\lambda_{\text{Em}} = 490\text{-}500\text{ nm}$), thus providing the opportunity to develop a ratiometric probe for sensing interactions via resonance energy transfer. To check this possibility, we selected the sequence **DNA1** since it resulted in the brightest combination of ss and ds DNAs (Table 1, **DNA1-2**: $\Phi = 0.30$ and 0.50). Cy3 was selected as a FRET acceptor and was introduced in the complementary sequence at its 5'-end (**DNA9** – Tables 1 & S1-S2, Figures S6-S7, S11 & S13).⁸ Cy3 was chosen because of its large molar absorptivity ($\epsilon_{547\text{nm}} = 13.6 \times 10^4\text{ M}^{-1}\cdot\text{cm}^{-1}$) and the significant spectral overlap ($J(\lambda) = 3.7 \times 10^{15}\text{ M}^{-1}\cdot\text{cm}^{-1}\cdot\text{nm}^4$, Eq1 in experimental section) between its absorption and the donor's emission spectra which are mandatory properties for efficient resonance energy transfer (Figure 3).

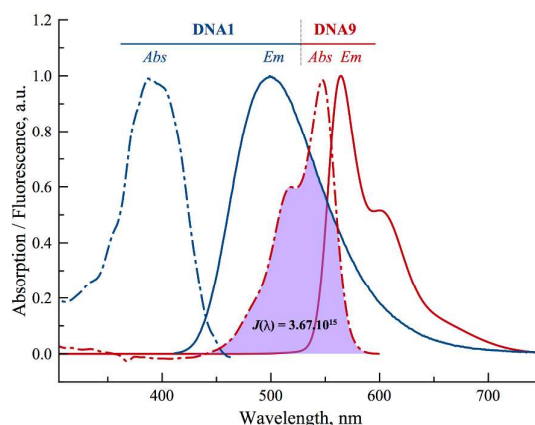


Figure 3. Absorption (dash-dotted lines) and emission (solid lines) spectra of ss **DNA1** (blue) and **DNA9** (red). The spectral overlap of the FRET pair considered in this study was colored in purple. Absorption and emission of **DNA1** and **DNA9** were normalized on their respective maximum.

The Förster distance R_0 is an important physical parameter that characterizes a FRET pair. It corresponds to the distance at which FRET efficiency is 50%. Thus, it is informative about the distance at which FRET can be detected.²⁵ The R_0 value was calculated for a randomly-oriented donor-acceptor pair and was found $\approx 51\text{ Å}$ (Eq2 in experimental section, $k^2 = 2/3$). This value is in the usual range of Förster distances of FRET pairs composed of organic dyes used for biological applications.^{1a} Furthermore, the absorption band of Cy3 centered at 548 nm is well-separated from the donor's one ($\Delta\lambda = 152\text{ nm}$) and the emission band in the yellow range (565 nm) has an appreciable quantum yield ($\Phi = 0.20$).²⁶ Additionally,

the fact that Cy3 does not absorb ($\epsilon_{390\text{ nm}} < 300\text{ m}^{-1}\cdot\text{cm}^{-1}$) at the wavelength where the 3HC donor is being excited is an important asset which dramatically increases the S/N ratio (Figures S13 & S17B).

The control and FRET experiments were performed with the single-labeled ds **DNA10** and double-labeled ds-**DNA11** obtained by annealing **DNA9** with the fully complementary wild-type and **DNA1** strands, respectively. In **DNA11**, the distance separating the donor and acceptor should be at least 27 Å assuming a 3.4 Å distance per base pair (B-DNA, Figure S11) and a stacked Cy3. By comparison to the wild-type duplex, the 2.4 °C rise of T_m supports that Cy3 stacks at the end of the DNA helix (Table 1, entry 10). When **DNA10** was excited at 396 nm, no emission was registered (Figure 4), confirming that Cy3 does not absorb at this wavelength. Contrastingly, when the duplex was excited at the absorption maximum of Cy3 (548 nm), the characteristic emission spectrum of Cy3 was observed. When it was irradiated at one quarter of its absorption maximum (490 nm), the shape of the emission did not change but the fluorescence intensity appeared to be one quarter of its maximum as expected (Figure 4). An efficient FRET was evidenced when the double-labeled **DNA11** was excited at the absorption maximum of the donor (396 nm).

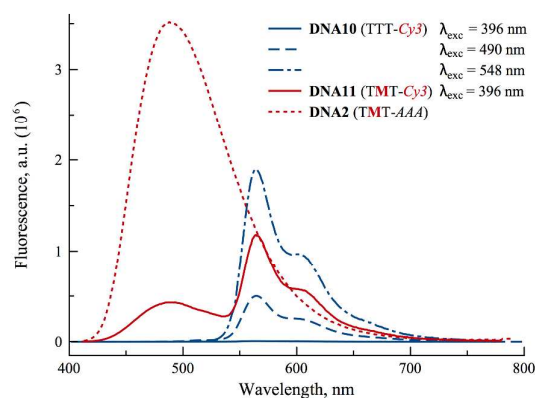


Figure 4. Emission spectra of Cy3-labeled **DNA10** (blue), **TMT-AAA DNA2** (dotted red), and **M-Cy3** double-labeled **DNA11** (solid red) duplexes at different excitation wavelengths at pH 7.0.

Indeed, the comparison of the emission of **DNA11** with the corresponding single-labeled ds **DNA10** and **DNA2** duplexes revealed a dramatic decrease of the emission intensity of the donor **M** at 490 nm together with a marked increase (over a factor >100) of the Cy3 emission intensity at 564 nm. The energy transfer efficiency was found to be 92 % for **DNA11** (Eq3 in experimental section). Using R_0 (51 Å) and E (92%), the distance r between the two dyes in **DNA11** was calculated to be about 34 Å (Eq4 in experimental section). It should be mentioned that this distance (34 Å) is likely overestimated, since Cy3 in the context of DNA stacks at the end of the helix. Furthermore, the fact that Cy3 stacks is known to affect the energy transfer efficiency, which can result in an error of up to 12 Å in the calculated r distance when using $k^2 = 2/3$.⁸ In our case, the difference was about 7 Å. Further evidence of FRET was provided by the excitation

spectra of the single and double-labeled **DNA10-11** (Figure S17). By collecting photons at 564 nm, only the spectrum registered from the double-labeled **DNA11** exhibited a band centered at 390 nm that perfectly fitted with the absorption spectrum of the donor (Figure S13). Since the donor emission locates in the blue edge and is well separated from the acceptor emission band, it permits an eased ratiometric detection of the FRET process.²⁷ Thus, by gradually increasing the concentration of **DNA9**, the energy transfer accompanying the formation of the duplex can be probed by a ratiometric two-color response (Figures 5 & S18). As expected, addition of 1 equivalent of **DNA9** was sufficient for completely inverting the intensity ratio at the two emission maxima from 0.5 to 3.4 resulting in about a 7-fold variation of the ratiometric response (Figures 5, S18 and S19). This saturation confirms that the observed FRET monitors the 1:1 stoichiometric process of duplex formation. Interestingly, this large variation in the ratio of the two emission maxima results in a change in the emission color of **DNA11** from cyan to yellow, offering a clear visualization of hybridization which might be useful for two-color imaging applications (Figure 5).

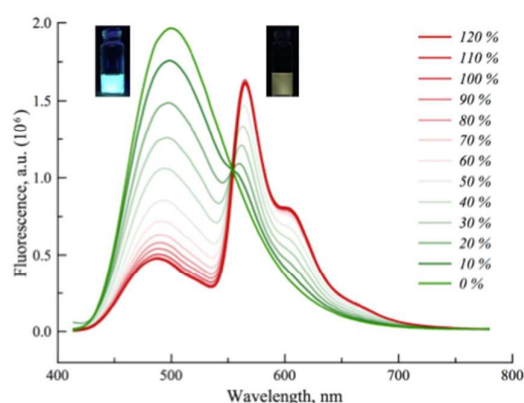


Figure 5. Fluorescence titration of **DNA1** upon addition of **DNA9** (from 0 to 1.2 equivalents) resulting in ratiometric emission changes due to FRET. Insets showed the color changes before (left: cyan cell) and after addition of 1 eq. of **DNA9** (right: yellow cell).

CONCLUSIONS

In summary, we reported the convergent synthesis and spectroscopic characterization of 15-mer sequences site-specifically labeled with a single-band emissive deoxyuridine analog. Based on a 2-thienyl-3-methoxychromone scaffold tethered to the C-5 position of an ethynyl uracil, the fluorophore (**M**) incorporated in DNA displays absorption in the visible range (ca. 400 nm) compatible with violet laser excitation, large absorption coefficient ($35.000 \text{ M}^{-1} \cdot \text{cm}^{-1}$), large Stokes shift ($\approx 100 \text{ nm}$), good quantum yields (up to 50%) and remarkable photostability. Using the key features of this fluorescent reporter, we developed an efficient FRET system where **M** acts as a donor in a first ODN and Cy3 in the complementary strand operates as an acceptor ($R_0 = 51 \text{ \AA}$). Fluorescence studies demonstrated a remarkable FRET efficiency, yielding to a net visual change in emission color from cyan to yellow upon hybridization. This FRET system

opens prospective applications for studying in real time duplex conformational changes that induce distance variation between the two FRET partners, as for instance on binding to DNA-bending proteins. Additionally, since the deoxyuridine conjugate absorbs in the violet and its emission locates in the green region (ca. 500 nm), the use of orange fluorescent proteins²⁸ as FRET acceptors will offer perspectives for two-color imaging of DNA/protein interactions.²⁹

EXPERIMENTAL SECTION

General methods: All reactions involving water-sensitive reagents were performed in oven-dried glassware under argon using dry solvents. The synthetic intermediates were beforehand co-evaporated twice with toluene and dried in *vacuo* before use. All chemical reagents were obtained from commercial sources and were used as supplied. Anhydrous solvents were obtained according to standard procedures.³⁰ The reactions were monitored by thin-layer chromatography (TLC, silica gel 60 F254 plates) and visualized both by UV radiation (254 & 365 nm) and by spraying with vanillin in ethanol containing H₂SO₄ followed by a subsequent warming with a heat gun. Column chromatography³¹ was performed with flash silica gel (40–63 mm). All NMR spectra (¹H, ¹³C, ²D) were recorded on 200 or 500 MHz spectrometers. ¹H NMR (200 and 500 MHz), ¹³C{¹H}NMR (50 and 125 MHz, recorded with complete proton decoupling), ³¹P{¹H}NMR (80 MHz, proton decoupling) spectra were obtained with samples dissolved in CDCl₃, CD₂Cl₂, CD₃OD, DMSO-*d*⁶, acetone-*d*₆, or CD₃CN with the residual solvent signals used as internal references: 7.26 ppm for CHCl₃, 5.32 ppm for CDHCl₂, 3.31 ppm for CD₂HOD, 2.50 ppm for (CD₃)(CD₂H)S(O), 2.05 ppm for (CD₃)(CD₂H)C(O), 1.94 ppm for CD₂HCN for ¹H NMR experiments, and 77.0 ppm for CDCl₃, 53.8 ppm for CD₂Cl₂, 49.0 ppm for CD₃OD, 39.4 ppm for (CD₃)₂S(O), 30.8 ppm for (CD₃)₂C(O) for ¹³C NMR experiments.³² Chemical shifts (δ) are given in ppm to the nearest 0.01 (¹H) or 0.1 ppm (¹³C). The coupling constants (*J*) are given in Hertz (Hz). The signals are reported as follows: (s=singlet, d=doublet, t=triplet, m=multiplet, br=broad). Assignments of ¹H and ¹³C NMR signals were achieved with the help of D/H exchange, COSY, DEPT, APT, HMQC, HSQC, HMBC experiments. Regular mass spectra (MS) were recorded with ESI in both positive and negative modes. High-resolution mass spectrometry was conducted on a hybrid quadrupole-Orbitrap mass spectrometer (combining quadrupole precursor selection with high-resolution and accurate-mass Orbitrap detection) using ESI ionization techniques. Supplementary data associated with this article, including the experimental protocols for the synthesis of intermediates **2** and **5-11**, the ¹H, ¹³C and (in part) ¹H–¹H COSY, ¹H–¹³C HMQC, ¹H–¹³C HSQC and ¹H–¹³C HMBC NMR spectra of all compounds, can be consulted in this *Supporting Information*. Systematic flavone and nucleobase nomenclatures are used below for the assignments of each spectrum. All solvents for absorption and fluorescence experiments were of spectroscopic grade. Absorption spectra were recorded on a spectrophotometer using 1cm quartz cells. Stock solution of the MTCU model **1** was prepared using dioxane. The samples used for spectroscopic measurements contained \approx 0.1% v/v of the stock solvent. Fluorescence spectra were recorded on a spectrofluorometer

with slits open to 2 nm. Excitation wavelength was used as mentioned in the corresponding experiments. Photostability studies were conducted in a 100 μ L fluorescence cell, excitation and emission slits were set to 4 nm. The concentrations of the samples were 2 μ M.

3-Methoxy-2-(5-bromothien-2-yl)-chromen-4-one (6). Compound **6** was synthesized as previously described.⁷

5'-O-(4,4'-Dimethoxytrityl)-5-iodo-2'-deoxyuridine (7b).³³ To a stirred solution of 5-iodo-2'-deoxyuridine **7** (1.00 g, 2.82 mmol) in dry pyridine (28 mL) were added triethylamine (795 μ L, 5.65 mmol, 2 eq.) and DMTrCl (1.00 g, 2.97 mmol, 1.05 eq.). The reaction mixture was stirred at rt for 1 d and then quenched with H₂O. The organic phase was extracted with CH₂Cl₂ (3 x), dried over Na₂SO₄, filtered and the volatiles were removed in vacuo. The resulting crude was purified by flash chromatography on silica gel eluted with CH₂Cl₂/MeOH (1:0 \rightarrow 96:4, v/v) to provide the desired compound **7b** as a white solid (1.82 g, 98 %). C₃₀H₂₉IN₂O₇ (656.46). *R*_f = 0.41 (CH₂Cl₂/MeOH, = 95:5). Mp= 128–129°C. ¹H-NMR (CD₂Cl₂, 200 MHz): δ = 2.27 (ddd, ²*J*=13.6 Hz, ³*J*=7.6, 6.0 Hz, 1H, H2'_A), 2.45 (ddd, ²*J*=13.6 Hz, ³*J*=5.8, 2.8 Hz, 1H, H2'_B), 3.35 (d, ³*J*=3.4 Hz, 2H, H5'), 3.78 (s, 6H, OCH₃), 4.02–4.14 (m, 1H, H4'), 4.47–4.60 (m, 1H, H3'), 6.26 (dd, ³*J*=7.6, 5.8 Hz, 1H, H1'), 6.86 (d, ³*J*=8.7 Hz, 4H, H_{m-PhOMe}), 7.20–7.32 (m, 3H, H_{m-Ph}, H_{p-Ph}), 7.34 (d, ³*J*=8.7 Hz, 4H, H_{o-PhOMe}), 7.40–7.46 (m, 2H, H_{o-Ph}), 8.09 (s, 1H, H6), 8.99 (NH); ¹³C-NMR (CD₂Cl₂, 50 MHz): δ = 41.7 (C2'), 55.7 (OMe), 64.0 (C5'), 68.8 (C5), 72.6 (C3'), 86.1 (C1'), 87.0 (C4'), 87.3 (5'-O-C_{IV}), 113.7 (C_{m-PhOMe}), 127.4 (C_{p-Ph}), 128.4 (C_{m-Ph}), 128.5 (C_{o-Ph}), 130.4 (C_{o-PhOMe}), 130.5 (C_{o-PhOMe}), 135.8 (C_{i-PhOMe}), 136.0 (C_{i-PhOMe}), 144.9 (C6), 145.0 (C_{i-Ph}), 150.6 (C2), 159.2 (C_{p-PhOMe}), 160.8 (C4); MS (ESI⁺, MeOH) *m/z*: 679.3 [M+Na]⁺, 695.3 [M+K]⁺.

5'-O-(4,4'-Dimethoxytrityl)-5-iodo-3'-O-triethylsilyl-2'-deoxyuridine (8). To a stirred solution of **7b** (1.60 g, 2.44 mmol) in dry DMF (12 mL), previously cooled down to 0 °C, were sequentially added triethylamine (1.24 mL, 8.77 mmol, 3.6 eq.), DMAP (90 mg, 0.73 mmol, 0.3 eq.) and Et₃SiCl (496 μ L, 2.93 mmol, 1.2 eq.). The reaction mixture was stirred at rt for 4 h and then carefully quenched with aq. NH₄Cl. The organic phase was extracted with CH₂Cl₂ (3 x), dried over MgSO₄, filtered and reduced *in vacuo*. The residue was purified by flash chromatography on silica gel eluted with toluene/Et₂O (95:5 \rightarrow 67:33, v/v) to provide the desired compound **8** as a light yellow foam (1.52 g, 82 %). C₃₆H₄₃IN₂O₇Si (770.73). *R*_f = 0.62 (toluene/Et₂O = 4:1). ¹H-NMR (CD₂Cl₂, 200 MHz): δ = 0.53 (q, ³*J*=7.8 Hz, 3H, CH₃), 0.89 (t, ³*J*=7.8 Hz, 2H, CH₂), 2.10–2.23 (m, 1H, H2'_A), 2.31–2.42 (m, 1H, H2'_B), 3.26 (dd, ²*J*=10.9 Hz, ³*J*=3.4 Hz, 1H, H5'_A), 3.36 (dd, ²*J*=10.9 Hz, ³*J*=2.9 Hz, 1H, H5'_B), 3.78 (s, 6H, OMe), 3.98–4.02 (m, 1H, H4'), 4.39–4.44 (m, 1H, H3'), 6.24 (dd, ³*J*=7.7, 5.7 Hz, 1H, H1'), 6.85 (d, ³*J*=8.8 Hz, 4H, H_{m-PhOMe}), 7.12–7.28 (m, 3H, H_{m-Ph}, H_{p-Ph}), 7.34 (d, ³*J*=8.8 Hz, 4H, H_{o-PhOMe}), 7.40–7.46 (m, 2H, H_{o-Ph}), 8.14 (s, 1H, H6), 8.72 (NH); ¹³C-NMR (CD₂Cl₂, 50 MHz): δ = 4.9 (CH₂), 6.8 (CH₃), 42.3 (C2'), 55.6 (OMe), 63.6 (C5'), 68.4 (C5), 72.8 (C3'), 86.2 (C1'), 87.3 (5'-O-C_{IV}), 87.8 (C4'), 113.7 (C_{m-PhOMe}), 127.3 (C_{p-Ph}), 128.4 (C_{o-Ph}), 128.4 (C_{m-Ph}), 130.4 (C_{o-PhOMe}), 130.5 (C_{o-PhOMe}), 135.8 (C_{i-PhOMe}), 135.9 (C_{i-PhOMe}), 144.9 (C6),

145.0 (C_{i-Ph}), 150.2 (C2), 159.2 ($C_{p-PhOMe}$), 160.5 (C4); MS (ESI⁺, MeOH) m/z : 793.4 [M+Na]⁺, 809.3 [M+K]⁺. HRMS (ESI⁺): m/z calcd for $C_{36}H_{43}IN_2NaO_7Si$: 793.1776 [M+Na]⁺; found 793.1767.

5'-O-(4,4'-Dimethoxytrityl)-5-trimethylsilylethynyl-3'-O-triethylsilyl-2'-deoxyuridine (9). To a stirred solution of **8** (1.40 g, 1.82 mmol, previously azeotropically coevaporated with dry toluene) in DMF (18 mL) under argon, were sequentially added TMS-acetylene (389 μ L, 2.73 mmol, 1.5 eq.), triethylamine (1.28 mL, 9.08 mmol, 5 eq.) and CuI (28 mg, 8 mol%)/PdCl₂(PPh₃)₂ (103 mg, 8 mol%) all together. The reaction mixture was warmed up to 55 °C for 3 h. The volatiles were removed *in vacuo* and the residue was purified by flash chromatography on silica gel eluted with toluene/Et₂O (95:5 → 66:34, v/v) to provide the desired compound **9** as a light yellow foam (1.23 g, 91 %). $C_{41}H_{52}N_2O_7Si_2$ (741.03). R_f = 0.62 (pentane/Et₂O = 1:2). ¹H-NMR (CDCl₃, 200 MHz): δ = -0.03 (s, 9H, SiMe₃), 0.51 (q, ³ J =7.8 Hz, 9H, CH₃), 0.88 (t, ³ J =7.8 Hz, 6H, CH₂), 2.03–2.17 (m, 1H, H2'_A), 2.37 (ddd, ² J =13.0 Hz, ³ J =5.6 Hz, ⁴ J =1.8 Hz, 1H, H2'_B), 3.22 (dd, ² J =10.8 Hz, ³ J =3.4 Hz, 1H, H5'_A), 3.45 (dd, ² J =10.8 Hz, ³ J =2.7 Hz, 1H, H5'_B), 3.79 (s, 3H, OMe), 3.98–4.04 (m, 1H, H4'), 4.26–4.34 (m, 1H, H3'), 6.28 (dd, ³ J =8.0, 5.4 Hz, 1H, H1'), 6.85 (d, ³ J =8.8 Hz, 4H, H_{m-PhOMe}), 7.15–7.32 (m, 3H, H_{m-Ph}, H_{p-Ph}), 7.35 (d, ³ J =8.8 Hz, 4H, H_{o-PhOMe}), 7.40–7.49 (m, 2H, H_{o-Ph}), 8.11 (s, 1H, H6); 8.94 (NH); ¹³C-NMR (CDCl₃, 50 MHz): δ = -0.4 (SiMe₃), 4.5 (SiCH₂), 6.6 (SiCH₂C≡CH₃), 42.0 (C2'), 55.2 (OMe), 63.2 (C5'), 72.5 (C3'), 86.0 (C1'), 86.9 (5'-O-C_{1V}), 87.6 (C4'), 94.8 (C≡C-TMS), 99.5 (C≡C-TMS), 100.3 (C5), 113.3 (C_{m-PhOMe}), 126.9 (C_{p-Ph}), 127.9 (C_{o-Ph}), 128.0 (C_{m-Ph}), 129.9 (C_{o-PhOMe}), 135.4 (C_{i-PhOMe}), 135.6 (C_{i-PhOMe}), 142.8 (C6), 144.4 (C_{i-Ph}), 149.0 (C2), 158.5 (C_{p-PhOMe}), 161.3 (C4); MS (ESI⁺, MeOH) m/z : 763.5 [M+Na]⁺, 779.5 [M+K]⁺. HRMS (ESI⁺): m/z calcd for $C_{41}H_{52}N_2NaO_7Si_2$: 763.3205 [M+Na]⁺; found 763.3192.

5'-O-(4,4'-Dimethoxytrityl)-3-N-(4-methylbenzoyl)-5-trimethylsilylethynyl-3'-O-triethylsilyl-2'-deoxyuridine (9b). To a stirred solution of **9** (1.19 g, 1.61 mmol) in dry acetonitrile (16 mL), previously cooled down to 0 °C, were sequentially added triethylamine (633 μ L, 4.50 mmol, 2.8 eq.) and toluoyl chloride (297 μ L, 2.25 mmol, 1.4 eq.). The reaction mixture was stirred at rt overnight and then carefully quenched with aq. NH₄Cl. The organic phase was extracted with CH₂Cl₂ (3 x), dried over MgSO₄, filtered and reduced *in vacuo*. The residue was purified by flash chromatography on silica gel eluted with toluene/Et₂O (99.5:0.5 → 96.5:3.5, v/v) to provide the desired compound **9b** as a beige foam (1.23 g, 89 %). $C_{49}H_{58}N_2O_8Si_2$ (859.16). R_f = 0.34 (toluene/Et₂O = 98:2). ¹H-NMR (CDCl₃, 200 MHz): δ = -0.00 (s, 9H, SiMe₃), 0.53 (q, ³ J =7.8 Hz, 9H, CH₃), 0.89 (t, ³ J =7.8 Hz, 6H, CH₂), 2.11–2.25 (m, 1H, H2'_A), 2.34–2.39 (m, 1H, H2'_B), 2.44 (s, 3H, *p*-CH₃), 3.27 (dd, ² J =10.8 Hz, ³ J =3.6 Hz, 1H, H5'_A), 3.41 (dd, ² J =10.8 Hz, ³ J =3.0 Hz, 1H, H5'_B), 3.79 (s, 3H, OMe), 4.00–4.09 (m, 1H, H4'), 4.31–4.41 (m, 1H, H3'), 6.23 (dd, ³ J =8.0, 5.6 Hz, 1H, H1'), 6.88 (d, ³ J =8.8 Hz, 4H, H_{m-PhOMe}), 7.13–7.31 (m, 3H, H_{m-Ph}, H_{p-Ph}), 7.33 (d, ³ J =8.2 Hz, ⁴ J =0.6 Hz, 2H, H_{m-Tol}), 7.38 (dd, ³ J =8.8 Hz, ⁴ J =0.8 Hz, 4H, H_{o-PhOMe}), 7.49 (dd, ³ J =8.4 Hz, ⁴ J =1.4 Hz, 2H, H_{o-Ph}), 7.81 (d, ³ J =8.2 Hz, 2H, H_{o-Tol}), 8.17 (s, 1H, H6); ¹³C-NMR (CDCl₃, 50

MHz): δ = -0.4 (SiMe₃), 4.9 (SiCH₂), 6.8 (SiCH₂CH₃), 22.0 (*p*-CH₃), 42.4 (C2'), 55.6 (OMe), 63.6 (C5'), 72.9 (C3'), 86.8 (C1'), 87.3 (5'-O-C_{IV}), 88.1 (C4'), 95.1 (C≡C-TMS), 100.0 (C≡C-TMS), 100.5 (C5), 113.6 (C_m-PhOMe), 127.3 (C_p-Ph), 128.3 (C_o-Ph), 128.4 (C_m-Ph), 129.0 (C_i-Tol), 130.3 (C_o-PhOMe), 130.4 (C_m-Tol), 130.9 (C_o-Tol), 135.9 (C_i-PhOMe), 142.9 (C6), 145.0 (C_i-Ph), 147.5 (C_p-Tol), 148.6 (C2), 159.1 (C_p-PhOMe), 160.9 (C4), 168.2 (C(O)-Tol); MS (ESI⁺, MeOH) *m/z*: 881.6 [M+Na]⁺, 897.6 [M+K]⁺. HRMS (ESI⁺): *m/z* calcd for C₄₉H₅₈N₂NaO₈Si₂: 881.3624 [M+Na]⁺; found 881.3601.

5'-O-(4,4'-Dimethoxytrityl)-3-N-(4-methylbenzoyl)-5-ethynyl-2'-deoxyuridine (10).²¹ To a stirred solution of **9b** (1.90 g, 2.21 mmol) in THF (22 mL), previously cooled down to 0 °C, was portionwise added Et₄NF.H₂O (2.00 g, 13.27 mmol, 6 eq.). The reaction mixture was stirred at rt for 1.5 h and then carefully quenched with aq. NH₄Cl. The organic phase was extracted with Et₂O (3 x), dried over MgSO₄, filtered and reduced *in vacuo*. The residue was purified by flash chromatography on silica gel eluted with toluene/Et₂O (93:7 → 1:1, v/v) to provide the desired compound **10** as a light yellow foam (1.23 g, 83 %). C₄₀H₃₆N₂O₈ (672.72). *R_f* = 0.22 (toluene/Et₂O = 7:2). ¹H-NMR (CD₂Cl₂, 200 MHz): δ = 2.25–2.43 (m, 1H, H2'_A), 2.44 (s, 3H, *p*-CH₃), 2.44–2.55 (m, 1H, H2'_B), 2.97 (s, 1H, C≡CH), 3.32 (dd, ²*J*=10.8 Hz, ³*J*=3.0 Hz, 1H, H5'_A), 3.41 (dd, ²*J*=10.8 Hz, ³*J*=3.4 Hz, 1H, H5'_B), 3.80 (s, 3H, OMe), 4.03–4.12 (m, 1H, H4'), 4.52–4.62 (m, 1H, H3'), 6.24 (dd, ³*J*=7.2, 6.0 Hz, 1H, H1'), 6.89 (d, ³*J*=8.6 Hz, 4H, H_m-PhOMe), 7.20–7.31 (m, 3H, H_m-Ph, H_p-Ph), 7.33 (d, ³*J*=8.1 Hz, 2H, H_m-Tol), 7.39 (d, ³*J*=8.6 Hz, 4H, H_o-PhOMe), 7.48 (dd, ³*J*=8.2 Hz, ⁴*J*=1.4 Hz, 2H, H_o-Ph), 7.81 (d, ³*J*=8.1 Hz, 2H, H_o-Tol), 8.21 (s, 1H, H6); ¹³C-NMR (CD₂Cl₂, 50 MHz): δ = 22.0 (*p*-CH₃), 41.9 (C2'), 55.6 (OMe), 63.8 (C5'), 72.4 (C3'), 74.4 (C≡CH), 82.4 (C≡CH), 86.6 (C1'), 87.1 (C4'), 87.5 (5'-O-C_{IV}), 99.3 (C5), 113.7 (C_m-PhOMe), 127.3 (C_p-Ph), 128.3 (C_o-Ph), 128.5 (C_m-Ph), 128.8 (C_i-Tol), 130.4 (C_m-Tol), 130.4 (C_o-PhOMe), 130.9 (C_o-Tol), 135.7 (C_i-PhOMe), 136.0 (C_i-PhOMe), 144.0 (C6), 145.0 (C_i-Ph), 147.7 (C_p-Tol), 148.6 (C2), 159.2 (C_p-PhOMe), 161.0 (C4), 168.1 (C(O)-Tol); MS (ESI⁺, MeOH) *m/z*: 695.5 [M+Na]⁺ 711.5 [M+K]⁺. HRMS (ESI⁺): *m/z* calcd for C₄₀H₃₆N₂NaO₈: 695.2364 [M+Na]⁺; found 695.2357.

5'-O-(4,4'-Dimethoxytrityl)-3-N-(4-methylbenzoyl)-5-(5-(3-Methoxy-4-oxo-chromen-2-yl)thien-2-yl)ethynyl-2'-deoxyuridine (11). To a stirred solution of **10** (300 mg, 0.45 mmol) and **6** (206 mg, 0.58 mmol, 1.3 eq) in THF (10 mL) under argon, were sequentially added triethylamine (311 μL, 2.23 mmol, 5 eq), and CuI (6 mg, 7 mol%)/PdCl₂(PPh₃)₂ (22 mg, 7 mol%) all together. The reaction mixture was warmed to 55 °C for 2 h. The volatiles were removed *in vacuo* and the residue was purified by flash chromatography on silica gel eluted with toluene/EA (93:7 → 3:2, v/v) to provide the desired compound **11** as a yellow foam (276 mg, 67 %). C₅₄H₄₄N₂O₁₁S (929.0). *R_f* = 0.38 (toluene/EA = 7:3). ¹H-NMR (CDCl₃, 200 MHz): δ = 2.39–2.49 (m, 1H, H2'_A), 2.43 (s, 3H, *p*-CH₃), 2.58 (ddd, ²*J*=13.6 Hz, ³*J*=5.8, 2.9 Hz, 1H, H2'_B), 3.37–3.51 (m, 2H, H5'), 3.73 (s, 3H, OMe), 3.74 (s, 3H, OMe), 3.97 (s, 3H, 3''-OMe), 4.10–4.19 (m, 1H, H4'), 4.59–4.71 (m, 1H, H3'), 6.35 (dd, ³*J*=5.0, 4.0 Hz, 1H, H1'), 6.82 (d, ³*J*=8.8 Hz, 2H, H_m-PhOMe), 6.84 (d, ³*J*=8.8 Hz, 2H, H_m-PhOMe), 6.87 (d, ³*J*=4.0 Hz, 1H, H3-thioph.), 7.15–7.35 (m, 6H, H6'', H_m-Tol, H_m-Ph, H_p-Ph), 7.37 (d, ³*J*=8.8 Hz, 4H, H_o-PhOMe), 7.42–

7.51 (m, 3H, H_{o-Ph} , $H8''$), 7.63–7.72 (m, 1H, $H7''$), 7.69 (d, $^3J=4.0$ Hz, 1H, $H4$ -thioph.), 7.85 (d, $^3J=8.2$ Hz, 2H, H_{o-Tol}), 8.22 (dd, $^3J=8.0$ Hz, $^4J=1.4$ Hz, 1H, $H5''$); 8.37 (s, 1H, $H6$); ^{13}C -NMR ($CDCl_3$, 50 MHz): δ = 21.9 ($p-CH_3$), 41.9 ($C2'$), 55.2 (OMe), 59.7 (OMe), 63.4 ($C5'$), 72.2 ($C3'$), 86.4 ($C1'$), 86.6 (Th- $\underline{C}\equiv C$ -), 86.9 (Th- $\underline{C}\equiv C$ -), 86.9 ($C4'$), 87.2 ($5'-O-C_{IV}$), 99.8 ($C5$), 113.4 ($C_{m-PhOMe}$), 117.7 ($C8''$), 124.2 ($C10''$), 124.8 ($C6''$), 125.7 ($C5''$), 127.1 (C_{p-Ph}), 127.9 (C_{o-Ph}), 128.1 (C_{m-Ph}), 128.1 (Th- $\underline{C}\equiv C$ -), 128.5 (C_{i-Tol}), 128.9 (Th4), $\square\square\square$ 129.8 (C_{m-Tol}), 130.0 ($C_{o-PhOMe}$), 130.7 (C_{o-Tol}), 132.4 ($C2''$ -Th), 132.6 (Th3), 133.6 ($C7''$), 135.3 ($C_{i-PhOMe}$), 135.5 ($C_{i-PhOMe}$), 138.8 ($C3''$), 142.3 ($C6$), 144.2 (C_{i-Ph}), 146.8 (C_{p-Tol}), 148.1 ($C2$), 150.6 ($C2''$), 154.7 ($C9''$), 158.6 ($C_{p-PhOMe}$), 160.2 ($C4$), 167.5 ($\underline{C}(O)$ -Tol), 173.9 ($C4''$); MS (ESI^+ , MeOH) m/z : 950.9 $[M+Na]^+$, 966.9 $[M+K]^+$. HRMS (ESI^+): m/z calcd for $C_{54}H_{44}N_2NaO_{11}S$: 951.2558 $[M+H]^+$; found 951.2531.

5'-O-(4,4'-Dimethoxytrityl)-3-N-(4-methylbenzoyl)-5-(5-(3-Methoxy-4-oxo-chromen-2-yl)thien-2-yl)ethynyl-2'-deoxyuridine, 3'-[(2-cyanoethyl)-N,N-diisopropyl]-phosphoramidite (2). To a stirred solution of **11** (280 mg, 0.301 mmol, beforehand azeotropically coevaporated with dry toluene) in CH_2Cl_2 (3 mL), previously cooled down to 0 °C, were sequentially added DIPEA (212 μ L, 1.206 mmol, 4 eq.) and 2-cyanoethyl-N,N-diisopropylchlorophosphoramidite (136 μ L, 0.603 mmol, 2 eq.). The reaction mixture was stirred at rt for 1 h. The volatiles were removed *in vacuo* and the residue was purified by flash chromatography on silica gel eluted with toluene/EtOAc (95:5 \rightarrow 65:35, v/v) to provide the desired compound **2** as a yellow foam (230 mg, 68 %). $C_{63}H_{61}N_4O_{12}PS$ (1129.22). R_f = 0.48 (toluene/EA = 8:2). 1H -NMR (CD_3CN , 200 MHz): δ = 1.06–1.19 (m, 12H, $N(CH(CH_3)_2)_2$), 2.45 (m, 3H, $p-CH_3$), 2.52–2.68 (m, 4H, $H2'$, $-CH_2CN$), 3.35–3.43 (m, 2H, $H5'$), 3.52–3.67 (m, 2H, $N(CH(CH_3)_2)_2$), 3.70 (s, 3H, OMe), 3.71 (s, 3H, OMe), 3.74–3.82 (m, 1H, $POCH_2-$), 3.93 (s, 3H, $3''$ -OMe), 4.16–4.23 (m, 1H, $H4'$), 4.68–4.86 (m, 1H, $H3'$), 6.13 (dd, $^3J=7.2$, 6.2 Hz, 1H, $H1'$), 6.16 (dd, $^3J=7.6$, 7.4 Hz, 1H, $H1'$), 6.84 (d, $^3J=8.8$ Hz, 2H, $H_{m-PhOMe}$), 6.86 (d, $^3J=8.8$ Hz, 2H, $H_{m-PhOMe}$), 6.96 (d, $^3J=4.0$ Hz, $H3$ -thioph.), 7.14–7.31 (m, 3H, H_{m-Ph} , H_{p-Ph}), 7.35–7.43 (m, 3H, H_{m-Tol} , $H6''$), 7.41 (d, $^3J=8.8$ Hz, 4H, $H_{o-PhOMe}$), 7.47–7.54 (m, 2H, H_{o-Ph}), 7.63 (d, $^3J=7.6$ Hz, $H8''$), 7.76 (ddd, $^3J=8.6$, 7.0 Hz, $^4J=1.6$ Hz, 1H, $H7''$), 7.80 (d, $^3J=4.0$ Hz, 1H, $H4$ -thioph.), 7.94 (d, $^3J=8.2$ Hz, 2H, H_{o-Tol}), 8.20 (dd, $^3J=8.0$ Hz, $^4J=1.6$ Hz, 1H, $H5''$); 8.38 (s, 1H, $H6$), 8.40 (s, 1H, $H6$); ^{31}P -NMR (CD_3CN , 81 MHz): δ = 148.0, 148.1. HRMS (ESI^+): m/z calcd for $C_{63}H_{61}N_4NaO_{12}PS$: 1151.3637 $[M+H]^+$; found 1151.3665.

ODN synthesis and purification. The ODN synthesis was performed on an Expedite 8900 DNA synthesizer using the “trityl off” mode and ultra-mild Pac phosphoramidite chemistry on a 0.2 μ mol scale involving dT, Ac-dC, Pac-dA, and dmf-dG or iPr-Pac-dG as standard phosphoramidites. The classical DNA assembly protocol “DMT-off” was used except for the following modifications: 5-Ethylthio-1H-tetrazole (ETT) was used as activating agent; Pac-anhydride was used for capping; a longer coupling time (1200 s) was applied to the 3HC phosphoramidite. Non-labeled ODNs used as wild-type sequences were purchased from a commercial supplier. The ODNs were cleaved from the solid support and deprotected

with concentrated aqueous ammonia at room temperature for 12 h. The ODNs were analyzed (0.5 mL/min) and purified (2.5 mL/min) by RP HPLC (including a Photodiode Array Detector) using analytical and semi-preparative C18 columns (300 × 4.60 mm and 250 × 10 mm, 5 μm particle size, 100Å). The following gradient system was used: 100 % A → (30 min) → 60 % A / 40 % B → (5 min) → 100 % B → (5 min) → 100 % A with A=Buffer pH 7.0 (1.9 L of deionized water, 160 mL acetonitrile, 28 mL triethylamine, 12 mL of acetic acid) and B=0.2 CH₃CN:0.8 Buffer.

MALDI-TOF/TOF analysis of ODNs. Dibasic Ammonium Citrate (DAC) (98% capillary GC), acetonitrile (HPLC grade) ultrapure 3-Hydroxypicolinic Acid (3-HPA) MALDI matrix and C4 pipette tips (Zip-Tip) were purchased from commercial suppliers. The samples (500 pmol) were diluted to 10 μL of water and were desalted with a C4 pipette Tips (Zip-tip). The Zip-tip was activated before use with 2 × 5 μL of water: CH₃CN (50:50) and 2 × 5 μL of DAC (50 mg/mL diluted in water). The 10 μL of the ODN solution were loaded on Zip-tip by drawing and expelling ten times. Next, the zip-tip was washed with 3 × 5 μL of DAC (50 mg/mL) and 3 × 5 μL of water. Elution was performed with 1.5 μL of 3-HPA matrix (80 mg/mL, 50:50 CH₃CN:DAC) directly on MALDI plate. The ODN profiles were obtained on a MALDI-TOF/TOF mass spectrometer in reflector mode with external calibration mixture (cal Mix 1+2). MALDI-TOF/TOF-MS analysis: MS spectra were recorded manually in a mass range of 500-6000 Da resulting from 400 laser shots of constant intensity fixed at 6200.

Preparation of the samples. The ODNs were prepared in cacodylate buffer pH 7.0: 10 mM cacodylate, 150 mM NaCl. Solutions of the single-strand solutions were prepared by mixing 400 μL of a stock solution of 20 mM cacodylate buffer solution pH 7.0, 80 μL of 1.5 M NaCl solution, 25 μL of 64 μM ssODN and 295 μL of deionized water. Double-strand solutions were prepared by mixing 400 μL of a stock solution of 20 mM cacodylate buffer solution pH 7.0, 80 μL of 1.5 M NaCl solution, 25 μL of 64 μM ODN1, 25 μL of 64 μM ODN2 and 270 μL of deionized water.

Denaturation studies and melting. Melting curves were recorded by following the temperature-dependence of the absorbance changes of the sample in triplicate (2 μM concentration of each strand). Absorption spectra were recorded in a Peltier thermostated cell holder on a spectrophotometer. Wavelength for detection was 260 nm. The path length of the cell was 1 cm. The temperature range for denaturation measurements was 5–80 °C. Speed of heating was 0.3 °C/min. The buffer was 10 mM cacodylate, 150 mM NaCl, pH 7.0. The melting curves were converted into a plot of α versus temperature, where α represents the fraction of single strands in the duplex state. The melting temperatures were extracted from these curves after differentiation as described elsewhere.³⁴

Circular dichroism studies. Circular dichroism spectra were recorded with 2 μ M solution of the canonical dsDNA and labeled dsDNA (3HC (**M**) opposite **A**, **T**) in buffer pH 7.0 (10 mM cacodylate buffer, 150 mM NaCl) at 25 $^{\circ}$ C on a spectropolarimeter. Two maxima were observed in CD spectra, one negative at 249 nm and a positive one at 282 nm.

Absorbance and Fluorescence spectra. Absorption and fluorescence experiments were performed in triplicate in pH 7.0 cacodylate buffer (10 mM cacodylate buffer, 150 mM NaCl, 1mM EDTA). The absorption spectra were recorded on a spectrophotometer using 1 cm quartz cells at 20 $^{\circ}$ C. The fluorescence spectra were recorded on a spectrofluorometer using excitation and emission slits of 2 nm and were corrected at excitation and emission. They were taken with absorbance of about 0.05 at 20 $^{\circ}$ C at the excitation wavelength mentioned in the corresponding experiments. The quantum yields were corrected from the variation of the refractive index of the different solvents. FRET parameters (including energy transfer efficiency and rate constant, spectral overlap integral and Förster distance) were calculated according to equations 1 to 4.

The spectral overlap integral ($J(\lambda)$ in $M^{-1}.cm^{-1}.nm^4$) of the donor emission and the acceptor absorption were determined by using the equation:

$$J(\lambda) = \frac{\int_0^{\infty} F_D(\lambda)\epsilon_A(\lambda)\lambda^4 d\lambda}{\int_0^{\infty} F_D(\lambda)d\lambda} \quad (Eq1)$$

where $F_D(\lambda)$ is the fluorescence intensity of the donor in the wavelength range $[\lambda; \lambda + \Delta\lambda]$ and ϵ_A is the extinction coefficient of the acceptor at λ .

The Förster distance was calculated according to:

$$R_0 = 0.211 \sqrt[6]{(\kappa^2 n^{-4} Q_D J(\lambda))} \quad (Eq2)$$

where κ^2 describes the relative orientations in space of the transition dipoles of the donor and acceptor (usually assumed to be equal to 2/3, which is appropriate for dynamic random averaging of the donor and acceptor); n is the refractive index of the medium (1.4 for biomolecules in aqueous solution) and Q_D is the quantum yield of the donor in the absence of acceptor.

The efficiency of resonance energy transfer (E in %) was measured from the donor fluorescence quenching according to:

$$E = \left(1 - \frac{F_{DA}}{F_D}\right) \times 100 \quad (Eq3)$$

where F_D and F_{DA} are respectively, the relative fluorescence intensities in the absence and presence of the acceptor.

Finally, the donor-to-acceptor distance r is determined from:

$$r = R_0 \sqrt[6]{\frac{(1 - E)}{E}} \quad (Eq4)$$

ASSOCIATED CONTENT

Additional data associated with this article including the characterization (mass, NMR, absorption, fluorescence, and circular dichroism spectra) of the products and ODNs can be consulted in the Supporting Information. This material is available free of charge via the Internet at <http://pubs.acs.org>.

AUTHOR INFORMATION

Corresponding Author

*E-mail: benoit.michel@unice.fr, burger@unice.fr

ACKNOWLEDGEMENTS

This work was supported by the ANR (ANR-12-BS08-0003-02), PACA région (DNAfix- 2014-02862 and 2014-07199) and the FRM (DCM20111223038). We thank the FRM for the PhD grant for N.B., the French Government for the Master 2 grant to I.A.K. and CEFIPRA for the Raman-Charpak fellowship to K.G.

DEDICATION

Dedicated to the memory of Professor Guy Ourisson.

REFERENCES

- (1) (a) Lakowicz, J. R. In *Principles of Fluorescence Spectroscopy*, 3rd ed.; Springer: New York, 2006; pp. 443–475. (b) Valeur, B.; Berberan-Santos, M. N. In *Molecular Fluorescence: Principles and Application*, 2nd ed.; Wiley-VCH: Weinheim, 2012, p. 592. (c) Demchenko, A. P. In *Introduction to Fluorescence Sensing*, 2nd ed.; Springer: Heidelberg, 2015, p. 794. (d) Yuan, L.; Lin, W.; Zheng, K.; Zhu, S. *Acc. Chem. Res.* **2013**, *46*, 1462.
- (2) (a) Demchenko, A. P. In *Advanced Fluorescence Reporters in Chemistry and Biology III: Applications in Sensing and Imaging*; Springer-Verlag: Berlin, Heidelberg, 2011, p. 352. (b) Mason, W. T.; Gallin, J. I. *Fluorescent and Luminescent Probes for Biological Activity*, 2nd ed.; Academic Press: London, 1999, p. 647. (c) Brand, L.; Johnson, M. *Methods in Enzymology: Fluorescence Spectroscopy*, Academic Press: San Diego, 2008, 450, pp. 185–199.
- (3) (a) *General review on fluorescence techniques*: Ishikawa-Ankerhold, H. C.; Ankerhold, R.; Drummen, G. P. C. *Molecules* **2012**, *17*, 4047. *FRET applied to DNA, for reviews*: (b) Lilley, D. M. J.; Wilson, T. J. *Curr. Opin. Chem. Biol.* **2000**, *4*, 507. (c) Didenko, V. V. *BioTechniques* **2001**, *31*, 1106. (d) *Selected example on reversible RET*: Bälter, M.; Hammarson, M.; Remón, P.; Li, S.; Gale, N.; Brown, T.; Andréasson, J. *J. Am. Chem. Soc.* **2015**, *137*, 2444.

- (4) *FRET pair using a mega-Stokes shift dye as a donor (not applied to DNA labeling)*: (a) Nagy, K.; Orbán, E.; Bosze, S.; Kele, P. *Chem.–Asian. J.* **2010**, *5*, 773. (b) Cserép, G. B.; Enyedi, K. N.; Demeter, A.; Mező, G.; Kele, P. *Chem.–Asian. J.* **2013**, *8*, 494. (c) Mizuno, T.; Umezawa, K.; Shindo, Y.; Citterio, D.; Oka, K.; Suzuki, K. *J. Fluoresc.* **2013**, *23*, 1007. (d) Cao, C.; Liu, X.; Qiao, Q.; Zhao, M.; Yin, W.; Mao, D. *Chem. Comm.* **2014**, *50*, 15811. (e) Moriarty, R. D.; Martin, A.; Adamson, K.; O'Reilly, E.; Mollard, P.; Forster, R. J.; Keyes, T. E. *J. Microscopy* **2014**, *253*, 204.
- (5) (a) Giestas, L.; Petrov, V.; Baptista, P. V.; Lima, J. C. *Photochem. Photobiol. Sci.* **2009**, *8*, 1130. (b) Ehrenschwender, T.; Varga, B. R.; Kele, P.; Wagenknecht, H.-A. *Chem.–Asian J.* **2010**, *5*, 1761. (c) Giestas, L.; Lima, J. C.; Baptista, P. V. *J. Biotechnol.* **2011**, *154*, 199. (d) Cordeiro, M.; Giestas, L.; Lima, J. C.; Baptista, P. *J. Biotechnol.* **2013**, *168*, 90. (e) Akamatsu, K.; Shikazono, N. *Anal. Biochem.* **2013**, *433*, 171. (f) Akamatsu, K.; Shikazono, N.; Saito, T. *Radiat. Res.* **2015**, *183*, 105.
- (6) *Selected dye examples in ODNs presenting mega-Stokes shifts*: (a) Riedl, J.; Pohl, R.; Ernsting, N. P.; Orsag P.; Fojta, M. *Chem. Sci.* **2012**, *3*, 2797. (b) Weinberger, M.; Berndt, F.; Mahrwald, R.; Ernsting, N. P.; Wagenknecht, H.-A. *J. Org. Chem.* **2013**, *78*, 2589. (c) Riedl, J.; Pohl, R.; Rulišek, L.; Hocek, M. *J. Org. Chem.* **2012**, *77*, 1026. (d) Okamoto, A.; Tainaka, K.; Saito, I. *Bioconjugate Chem.* **2005**, *16*, 1105. (e) Kimura, T.; Kawai, K.; Majima, T. *Org. Lett.* **2005**, *7*, 5829. (f) Suzuki, A.; Kimura, K.; Ishioroshi, S.; Saito, I.; Nemoto, N.; Saito, Y. *Tetrahedron Lett.* **2013**, *54*, 2348. *No quantum yield provided*: (g) Jadhav, V. R.; Barawkar, D. A.; Ganesh, K. N. *J. Phys. Chem. B* **1999**, *103*, 7383.
- (7) Dziuba, D.; Karpenko, I. A.; Barthes, N. P. F.; Michel, B. Y.; Klymchenko, A. S.; Benhida, R.; Demchenko, A. P.; Mély, Y.; Burger, A. *Chem.–Eur. J.* **2014**, *20*, 1998.
- (8) (a) Moreira, B. G.; You, Y.; Owczarzy, R. *Biophys. Chem.* **2015**, *198*, 36. (b) Iqbal, A.; Arslan, S.; Okumus, B.; Wilson, T. J.; Giraud, G.; Norman, D. G.; Ha, T.; Lilley, D. M. J. *Proc. Natl. Acad. Sci. USA* **2008**, *105*, 11176.
- (9) *Two-fluorophore (radiative) FRET applied to nucleic acids; two-dye molecular beacon*: (a) Varghese, R.; Wagenknecht, H.-A. *Org. Biomol. Chem.* **2010**, *8*, 526. (b) Holzhauser, C.; Wagenknecht, H.-A. *Angew. Chem. Int. Ed.* **2011**, *50*, 7268. (c) Jockusch, S.; Martí, A. A.; Turro, N. J.; Li, Z.; Li, X.; Ju, J.; Stevens, N.; Akins, D. L. *Photochem. Photobiol. Sci.* **2006**, *5*, 493. (d) Socher, E.; Bethge, L.; Knoll, A.; Jungnick, N.; Herrmann, A.; Seitz, O. *Angew. Chem. Int. Ed.* **2008**, *47*, 9555. *Binary energy transfer*: (e) Ikeda, S.; Kubota, T.; Wang, D. O.; Yanagisawa, H.; Yuki, M.; Okamoto, A. *Org. Biomol. Chem.* **2011**, *9*, 6598. *Detection of RNA-Small Molecule Binding*: (f) (1) Xie, Y.; Dix, A. V.; Tor, Y. *J. Am. Chem. Soc.* **2009**, *131*, 17605.
- (10) Barthes, N. P. F.; Karpenko, I. A.; Dziuba, D.; Spadafora, M.; Auffret, J.; Demchenko, A. P.; Mély, Y.; Benhida, R.; Michel, B. Y.; Burger, A. *RSC Adv.* **2015**, *5*, 33536.
- (11) Smith, M. A.; Neumann, R. M.; Webb, R. A. *J. Heterocycl. Chem.* **1968**, *5*, 425.

- (12) Dziuba, D.; Benhida, R.; Burger, A. *Synthesis* **2011**, 2159.
- (13) (a) Asakura, J.-I.; Robins, M. J. *Tetrahedron Lett.* **1988**, 29, 2855. (b) Asakura, J.-I.; Robins, M. J. *J. Org. Chem.* **1990**, 55, 4928.
- (14) *From 5-ethynyluridines*: (a) Luoni, G.; McGuigan, C.; Andrei, G.; Snoeck, R.; De Clercq, E.; Balzarini, J. *Bioorg. Med. Chem. Lett.* **2005**, 15, 3791. (b) McGuigan, C.; Bidet, O.; Derudas, M.; Andrei, G.; Snoeck, R.; Balzarini, J. *Bioorg. Med. Chem.* **2009**, 17, 3025.
- (15) (a) *General review including N3-protection*: Beaucage, S. L.; Iyer, R. P. *Tetrahedron* **1992**, 48, 2223. (b) *N3-benzoylation*: Kumarasinghe, E. S.; Peterson, M. A.; Robins, M. J. *Tetrahedron Lett.* **2000**, 41, 8741.
- (16) Nesterova, I. V.; Erdem, S. S.; Pakhomov, S.; Hammer, R. P.; Soper, S. A. *J. Am. Chem. Soc.* **2009**, 131, 2432.
- (17) Melhuish, W. H. *J. Phys. Chem.* **1961**, 65, 229.
- (18) Ormson, S. M.; Brown, R. G.; Vollmer, F.; Rettig, W. *J. Photochem. Photobiol. A* **1994**, 81, 65.
- (19) Karstens, T.; Kobs, K. *J. Phys. Chem.* **1980**, 84, 1871.
- (20) (a) Dziuba, D.; Postupalenko, V. Y.; Spadafora, M.; Klymchenko, A. S.; Guérineau, V.; Mély, Y.; Benhida, R.; Burger, A. *J. Am. Chem. Soc.* **2012**, 134, 10209. (b) Sinkeldam, R. W.; Marcus, P.; Uchenik, D.; Tor, Y. *ChemPhysChem* **2011**, 12, 2260. (c) Sholokh, M.; Zamotaiev, O. M.; Das, R.; Postupalenko, V. Y.; Richert, L.; Dujardin, D.; Zaporozhets, O. A.; Pivovarenko, V. G.; Klymchenko, A. S.; Mély, Y. *J. Phys. Chem. B* **2015**, 119, 2585.
- (21) Barthes, N. P. F.; Gavvala, K.; Dziuba, D.; Bonhomme, D.; Karpenko, I. A.; Dabert-Gay, A. S.; Debayle, D.; Demchenko, A. P.; Benhida, R.; Michel, B. Y.; Mély, Y.; Burger, A. *J. Mater. Chem. C* **2016**, 4, 3010.
- (22) (a) Wilhelmsson, L. M. *Q. Rev. Biophys.* **2010**, 43, 159. (b) Sinkeldam, R. W.; Greco, N. J.; Tor, Y. *Chem. Rev.* **2010**, 110, 2579.
- (23) Kucherak, O. A.; Didier, P.; Mély, Y.; Klymchenko, A. S. *J. Phys. Chem. Lett.* **2010**, 1, 616.
- (24) (a) Kucherak, O. A.; Richert, L.; Mély, Y.; Klymchenko, A. S. *Phys. Chem. Chem. Phys.* **2012**, 14, 2292. (b) Sarkar, M.; Samanta, A. *J. Phys. Chem. B* **2007**, 111, 7027.
- (25) (a) Börjesson, K.; Preus, S.; El-Sagheer, A. H.; Brown, T.; Albinsson, B.; Wilhelmsson, L. Å. M. *J. Am. Chem. Soc.* **2009**, 131, 4288. (b) Teo, Y. N.; Kool, E. T. *Bioconjugate Chem.* **2009**, 20, 2371.
- (26) Berlier, J. E.; Rothe, A.; Buller, G.; Bradford, J.; Gray, D. R.; Filanoski, B. J.; Telford, W. G.; Yue, S.; Liu, J.; Cheung, C.-Y.; Chang, W.; □ Hirsch, J. D.; Beechem, J. M.; Haugland, R. P.; Haugland, R. P. *J. Histochem. Cytochem.* **2003**, 51, 1699.
- (27) (a) Demchenko, A. P. *J. Fluoresc.* **2010**, 20, 1099. (b) Demchenko, A. P. *J. Mol. Struct.* **2014**, 1077, 51.

- (28) Shaner, N. C.; Lin, M. Z.; McKeown, M. R.; Steinbach, P. A.; Hazelwood, K. L.; Davidson, M. W.; Tsien, R. Y. *Nat. Meth.* **2008**, *5*, 545.
- (29) Shvadchak, V. V.; Klymchenko, A. S.; de Rocquigny, H.; Mely, Y. *Nucl. Acids Res.* **2009**, *37*, e25.
- (30) Armarego W. L. F.; Chai, C. L. L. In *Purification of Laboratory Chemicals*, 7th ed.; Butterworth-Heinemann: Oxford, 2012; p. 1024.
- (31) Still, W. C.; Kahn, M.; Mitra, A. *J. Org. Chem.* **1978**, *43*, 2923.
- (32) (a) Gottlieb, H. E.; Kotlyar, V.; Nudelman, A. *J. Org. Chem.* **1997**, *62*, 7512. (b) Fulmer, G. R.; Miller, A.; Sherden, N. H.; Gottlieb, H. E. *Organometallics* **2010**, *29*, 2176.
- (33) Hansen, A. S.; Thalha mmer, A.; El-Sagheer, A. H.; Brown, T.; Schofield, C. J. *Bioorg. Med. Chem. Lett.* **2011**, *21*, 1181.
- (34) Breslauer, K. J. *Methods Enzymol.* **1995**, *259*, 221.

Graphical Abstract

1
2
3
4
5
6
7
8
9
10
11
12
13
14
15
16
17
18
19
20
21
22
23
24
25
26
27
28
29
30
31
32
33
34
35
36
37
38
39
40
41
42
43
44
45
46
47
48
49
50
51
52
53
54
55
56
57
58
59
60

